Ophiopogon japonicus polysaccharide reduces doxorubicin-induced myocardial ferroptosis injury by activating Nrf2/GPX4 signaling and alleviating iron accumulation

YONGTING CHEN[1,2*], LINLIN MA[2*], YUZHONG YAN[2], XIAOYING WANG[3], LIZHI CAO[2], YANFEI LI[2] and MING LI[4]

[1]Graduate School, Xinxiang Medical University, Xinxiang, Henan 453003, P.R. China; [2]Scientific Research Department, Shanghai University of Medicine and Health Sciences Affiliated Zhoupu Hospital, Shanghai 201318, P.R. China; [3]School of Life Sciences and Technology, Tongji University, Shanghai 200092, P.R. China; [4]Administration Office, East Hospital Affiliated to Tongji University, Shanghai 201318, P.R. China

Received June 20, 2024; Accepted October 8, 2024

DOI: 10.3892/mmr.2024.13401

Abstract. Doxorubicin (DOX) is a principal chemotherapeutic agent in the domain of oncological intervention. However, its clinical application is constrained due to its severe and irreversible side effects, particularly heart damage. Ferroptosis, characterized by iron accumulation and redox system imbalance, serves a key role in DOX-induced cardiotoxicity. *Ophiopogon japonicus* polysaccharide (OJP) exhibits diverse pharmacological activities, including cardiovascular protection, and anti-inflammatory, anti-oxidative and immune regulatory effects. However, the role and mechanism of OJP in DOX-mediated ferroptosis-triggered injury in cardiomyocytes remain elusive. The present study aimed to assess the effect of OJP on DOX-induced myocardial ferroptosis injury and to reveal its underlying anti-ferroptosis mechanism. The detection of myocardial injury markers, such as LDH, indicated that OJP can ameliorate myocardial damage. Additionally, western blot analyses reveal that OJP decreases the expression levels of the ferroptosis-related marker transferrin receptor 1 (TFR1) while simultaneously increasing expression levels of glutathione peroxidase 4 (GPX4) in a concentration-dependent manner. Furthermore, fluorescence probe assays demonstrate that OJP not only reduces iron accumulation and oxidative stress but also inhibits the production of lipid peroxidation, as evidenced by a decrease in malondialdehyde (MDA) levels measured. In addition, OJP simultaneously decreased ferroptosis by enhancing mitochondrial function. Mechanistically, OJP attenuated ferroptosis by upregulating the endogenous key antioxidant factor nuclear factor erythroid 2-related factor 2 (Nrf2), which in turn increased the expression of the downstream signaling molecule GPX4 and reduced the accumulation of the labile iron pool. Therefore, OJP may be a novel therapeutic intervention for DOX-induced ferroptosis-triggered myocardial injury.

Correspondence to: Professor Yanfei Li, Scientific Research Department, Shanghai University of Medicine and Health Sciences Affiliated Zhoupu Hospital, 1500 Zhouyuan Road, Pudong New Area, Shanghai 201318, P.R. China
E-mail: liyf@sumhs.edu.cn

Professor Ming Li, Administration Office, East Hospital Affiliated to Tongji University, 150 Jimo Road, Pudong New Area, Shanghai 201318, P.R. China
E-mail: lm0009@easthospital.cn

*Contributed equally

Key words: Ophiopogon japonicus polysaccharide, doxorubicin, cardiotoxicity, ferroptosis, Nrf2/GPX4 signaling pathway

Introduction

Doxorubicin (DOX), a potent chemotherapeutic agent, is widely used to treat several types of malignant tumors in clinical settings, including breast and lung cancer, and others (1). However, its non-targeted action limits its therapeutic application (2). DOX-induced cardiomyopathy (DIC) represents the most severe adverse reaction to DOX (3). It manifests as concentration-dependent, cumulative and potentially fatal myocardial injury, resulting in severe cardiomyopathy and heart failure (4,5).

Ferroptosis serves a pivotal role in the onset and progression of DIC (6). Ferroptosis refers to a programmed cell death mode characterized by excessive Fe^{2+} production and accumulation of lipid peroxides. It is characterized by redox system imbalance, leading to cell membrane destruction and subsequent cell death (7). Glutathione peroxidase 4 (GPX4), a key antioxidant enzyme, is involved in reducing lipid peroxides to non-toxic alcohols (8). DOX could downregulate GPX4, thus triggering ferroptosis by disrupting the antioxidant system (8). Transferrin receptor protein 1 (TFR1) serves a key role in ferroptosis by mediating the entry of Fe^{3+} into cells to be converted into Fe^{2+} (9). In addition, DOX increases TFR1 expression on the cell membrane, allowing the excessive accumulation of intracellular iron, triggering ferroptosis (10). Consequently, reducing ferroptosis during the application

of DOX in the treatment of malignant tumors is of importance (11).

Nuclear factor erythroid 2-related factor 2 (Nrf2) is involved in regulating ferroptosis in a direct or indirect manner via several pathways. The pathways include iron regulation, NADPH regeneration and the antioxidant pathway, and the modulation of mitochondrial function (12). Luo *et al* (13) demonstrated that astragaloside IV attenuated DOX-induced myocardial ferroptosis in rats by upregulating Nrf2. Furthermore, resveratrol alleviates ferroptosis via the p62/Nrf2 axis (14). Li *et al* (15) demonstrated that fisetin decreased myocardial ferroptosis by regulating the sirtuin 1/Nrf2 pathway. Therefore, Nrf2 upregulation could be an effective strategy to inhibit DOX-induced myocardial ferroptosis.

Ophiopogon japonicus polysaccharide (OJP), a major bioactive compound within *O. japonicus*, exhibits diverse pharmacological activities, including anti-inflammatory, antioxidant and immunomodulatory effects (16). Previous studies have suggested that OJP mitigates cardiac injury through several pathways (17,18). However, to the best of our knowledge, whether OJP attenuates DOX-induced myocardial ferroptosis has not been elucidated, and its underlying mechanism remains to be investigated.

The present study aimed to investigate whether OJP decreases ferroptosis by lowering iron buildup and lipid peroxidation. In addition, the inhibitory effect of OJP on ferroptosis by activating Nrf2 to upregulate the downstream GPX4 and decrease the accumulation of Fe^{2+} in the labile iron pool was also explored. Overall, the present study could provide a novel therapeutic strategy for mitigating DOX-induced myocardial ferroptosis injury.

Materials and methods

Cell culture. The human cardiomyocyte AC16 cell line was obtained from Ningbo Mingzhou Biotechnology Co., Ltd. (cat. no. MZ-4038). Cells were cultured in DMEM with high glucose (Shanghai Basal Media Technologies Co., Ltd.) supplemented with 10% fetal bovine serum (Gibco; Thermo Fisher Scientific, Inc.) and 1% penicillin/streptomycin solution (Biosharp Life Sciences) at 37˚C in a cell culture incubator with 5% CO_2. DOX, ML385 and ferrostatin-1 (Fer-1) were purchased from MedChemExpress (cat. nos. HY-15142, HY-100523 and HY-100579, respectively). OJP (purity, 98.50%) was obtained from Shanghai Winherb Medical Technology Co., Ltd. (cat. no. TDT017). DOX was utilized at 0.5 μM for 24 h to establish the myocardial ferroptosis injury model, while OJP was added (50, 100, 200 μg/ml) for 6 h. In addition, 5 μM Fer-1 or 10 μM ML385 were added for 6 h at 37˚C.

Cell viability assay. The viability of AC16 cells was assessed using a Cell Counting Kit-8 (CCK-8; Beyotime Institute of Biotechnology) assay. Briefly, cells (5,000 cells/well) were inoculated into 96-well culture plates and incubated overnight at 37˚C, followed by treatment with different concentrations of DOX (0.1, 0.5, 1.0, 2 μM) and OJP (50, 100, 200 μg/ml) for 24 h, or pretreated with OJP or Fer-1 (5 μM) for 6 h, followed by treatment with DOX at 0.5 μM for 24 h. Cells were washed once with PBS and then 10 μl CCK-8 solution was added, followed by incubation for 1 h at 37˚C. Finally, the absorbance in each well was measured at 450 nm using a microplate reader (cat. no. PT-3502PC, Beijing Potenov Technology Co. Ltd.).

Lactate dehydrogenase (LDH) detection. Following treatment as aforementioned, cell supernatant was obtained by centrifugation at room temperature 400 g for 5 min, mixed with LDH assay working solution (cat. no. C0016, Beyotime Institute of Biotechnology) and transferred to a 96-well plate. Subsequently, the plate was incubated at room temperature in the dark for an additional 30 min and the absorbance was measured at 490 nm using a microplate reader.

Creatine phosphokinase-MB (CK-MB) and cardiac troponin I (cTn-I) assessment. The levels of CK-MB and cTn-I were determined using the corresponding ELISA kits. Cells were treated as aforementioned. The supernatant was collected by centrifugation at 1,500 g for 20 min at room temperature. ELISA kits were used according to the manufacturer's instructions (cat. no. H197-1-1, cat. no. H149-2-1, Nanjing Jiancheng Bioengineering Institute). Following incubation for 30 min at room temperature, the plates were washed with detergent in the kits. After the addition of color developing and stop solutions, the absorbance was measured at 450 nm with a microplate reader.

Reactive oxygen species (ROS) level assessment. Cells (60,000 cells/well) were plated into 6-well culture plates and treated as aforementioned. 2'-7'-dichlorodihydrofluorescein diacetate (DCFH-DA; Beyotime Institute of Biotechnology) was diluted in serum-free DMEM and the appropriate volume (1 ml/well) of diluted DCFH-DA was added to each well after the culture medium was removed. Subsequently, the cells were incubated at 37˚C for 20 min. Following washing with serum-free DMEM three times, the cells were observed under a fluorescence microscope (Olympus Corporation). ImageJ2 (version 1.53, National Institutes of Health) was used in fluorescence intensity analysis. In addition, cells treated with OJP at 200 μg/ml for 6 h in the presence or absence of 10 μM ML385 were pretreated for 6 h and then molded at 37˚C. Single-cell suspensions were collected after three washes with PBS and analyzed using flow cytometry (Agilent NovoCyte Penteon, Agilent Technologies, Inc.). Analysis of flow cytometry results was performed with NovoExpress (version 1.4.1, Agilent Technologies, Inc.).

Western blot analysis. Following treatment as aforementioned, cells were washed three times with PBS and lysed with RIPA lysis buffer (cat. no. P0013C; Beyotime Institute of Biotechnology) supplemented with protease inhibitors for 30 min at 4˚C. The mixture was centrifuged at 12,000 x g for 30 min at 4˚C and the supernatant was then collected. Nuclear and Cytoplasmic Protein Extraction Kit (cat. no. P0027, Beyotime Institute of Biotechnology) was used to isolate nuclear and cytoplasmic proteins. After the cells were washed with PBS, cytoplasmic extraction reagent was added, the cells were lysed at 4˚C for 15 min, and then centrifuged at 4˚C for 16,000 g for 5 min to obtain the supernatant, which was cytoplasmic protein. The remaining precipitation was lysed at 4˚C

for 30 min after adding nuclear extraction reagent, and the supernatant was obtained after 10 min of centrifugation at 4˚C 16,000 g. The protein concentration was measured using the BCA Protein Quantification kit (cat. no. P0009, Beyotime Institute of Biotechnology). Proteins (35 μg/lane) was separated by 10% SDS-PAGE and then transferred to PVDF membranes. Following blocking with 5% non-fat powdered milk at room temperature for 1 h, the membranes were incubated with primary antibodies against TFR1 (1:500, cat. no. sc-393719, Santa Cruz Biotechnology, Inc.), GPX4 (1:1,000, cat. no. 30388-1-AP), Nrf2 (1:2,000, cat. no. 16396-1-AP), β-actin (1:5,000, cat. no. 66009-1-Ig, all Proteintech Group, Inc.) and histone H3 (1:2,000; cat. no. 9715S, Cell Signaling Technology, Inc.) overnight at 4˚C. Subsequently, the membranes were incubated with the corresponding HRP-conjugated secondary antibodies (1:5,000; cat. nos. sc-2357 and sc-525409, all Santa Cruz Biotechnology, Inc.) for 1 h at room temperature. Membranes were treated with Omni-ECL (cat. no. SQ201, Epizyme Biomedical Technology), the protein bands were visualized using the Tanon-4600 Chemiluminescence Imaging System (Tanon Science and Technology Co., Ltd.). The bands were analyzed using the ImageJ2 software (version 1.53, National Institutes of Health).

Fe^{2+} level detection. To measure the relative amount of intracellular Fe^{2+} following cell treatment as aforementioned. A FerroOrange fluorescent probe (cat. no. F374, Dojindo Molecular Technologies, Inc.) was utilized. Briefly, cells (65,000 cells/well) seeded into 6-well plates were washed three times with serum-free medium (DMEM, Shanghai Basal Media Technologies Co., Ltd.) followed by addition of 1 μmol/l Fe^{2+} detection working solution. Subsequently, cells were incubated in a 37˚C cell culture incubator for 30 min prior to examination under a fluorescence microscope (Olympus Corporation). The fluorescence intensity analysis was conducted using ImageJ2 (version 1.53, National Institutes of Health).

Malondialdehyde (MDA) content measurement. As MDA is the end product of lipid peroxidation (19), the degree of lipid peroxidation was evaluated by measuring MDA levels. Following cell lysis with Western and IP cell lysis buffer (cat. no. P0037, Beyotime Institute of Biotechnology), the protein concentration was measured using a BCA kit. The supernatant (12,000 g for 20 min at 4˚C) was mixed with MDA working solution (cat. no. S0131, Beyotime Institute of Biotechnology) and incubated at 100˚C for 15 min prior to cooling to room temperature. Following centrifugation at 1,000 x g for 10 min at room temperature, 200 μl supernatant was added into a 96-well plate. Finally, the absorbance in each well was measured at a wavelength of 532 nm with the microplate reader.

ATP content assessment. ATP content was detected using the Enhanced ATP Assay Kit (cat. no. S0027, Beyotime Institute of Biotechnology). The cell supernatant was obtained following cell lysis with ATP lysate (Beyotime Institute of Biotechnology). The relative light unit values were measured with a luminometer (SpectraMax iD5, Molecular Devices, Inc.) following mixing of 100 μl assay solution and 20 μl of each sample in a white background 96-well plate.

Mitochondrial membrane potential (MMP) assessment. An enhanced MMP assay kit with JC-1 (cat. no. C2003S, Beyotime Institute of Biotechnology) was used to evaluate the MMP. After the culture medium was removed, cells (60,000 cells/well) in the 6-well plate were supplemented with 1 ml DMEM, Shanghai Basal Media Technologies Co., Ltd.) and JC-1 staining solution. Subsequently, cells were incubated for 20 min at 37˚C. Cells were washed twice with JC-1 staining buffer and observed under a fluorescence microscope (Olympus Corporation). The fluorescence intensity analysis was performed utilizing ImageJ2 (version 1.53, National Institutes of Health).

Immunofluorescence staining. Cells (50,000 cells/well) were cultured with OJP at 200 μg/ml for 6 h followed by treatment with DOX at 0.5 μM for 24 h at 37˚C in 6-well plates, fixed with 4% paraformaldehyde for 15 min, and permeabilized with 0.1% Triton X-100 for 10 min and blocked with Immunol staining blocking buffer (cat. no. P0260, Beyotime Institute of Biotechnology) for 15 min at room temperature. Cells were incubated with Nrf2 antibody (1:2,000, cat. no. 16396-1-AP, Proteintech Group, Inc.) at 4˚C overnight, followed by incubation with the corresponding secondary antibody conjugated to Alexa Fluor® 488 (1:200, cat. no. ab150077, Abcam, Inc.) for 1 h in room temperature. Following washing with PBS, cells were stained with DAPI (cat. no. C1002, Beyotime Institute of Biotechnology) for 5 min and images were captured under a fluorescence microscope (Leica Microsystem) at room temperature. Image analyses were processed with the Leica Application Suite X (version 4.6.0, Leica Microsystem, Inc.).

Statistical analysis. All statistical analyses were performed using GraphPad Prism 8.0 software (Dotmatics). The results are presented as the mean ± SD of 3 independent experimental repeats. The differences among multiple groups were compared using one-way ANOVA followed by Dunnett's or Tukey's post hoc test. $P<0.05$ was considered to indicate a statistically significant difference.

Results

OJP protects against DOX-induced myocardial injury. DOX was utilized at a concentration of 0.5 μM for modeling, while OJP was administrated at concentrations of 50-200 μg/ml for pre-treatment. The specific grouping is depicted in Fig. 1A. To investigate the potential protective effects of OJP against DOX-induced cardiac cytotoxicity, a CCK-8 assay was performed. Initially, the optimal concentration of DOX was determined for model establishment. Following treatment with 0.5 μM DOX for 24 h, the cell viability was decreased to ~50% (Fig. 1B). Consequently, based on previous studies (14,20) and these preliminary experiments, a concentration of 0.5 μM DOX was chosen for further experiments. Subsequently, the effect of OJP on AC16 cell viability was assessed. OJP had no significant effect on cell viability, suggesting that OJP at 50-200 μg/ml had no cytotoxic effects on AC16 cells after 24 h of exposure (Fig. 1C). The ferroptosis inhibitor Fer-1 significantly inhibited DOX-mediated cell death, indicating that ferroptosis was involved in DOX-induced cell death (Fig. 1D). Additionally, OJP relieved DOX-induced cell

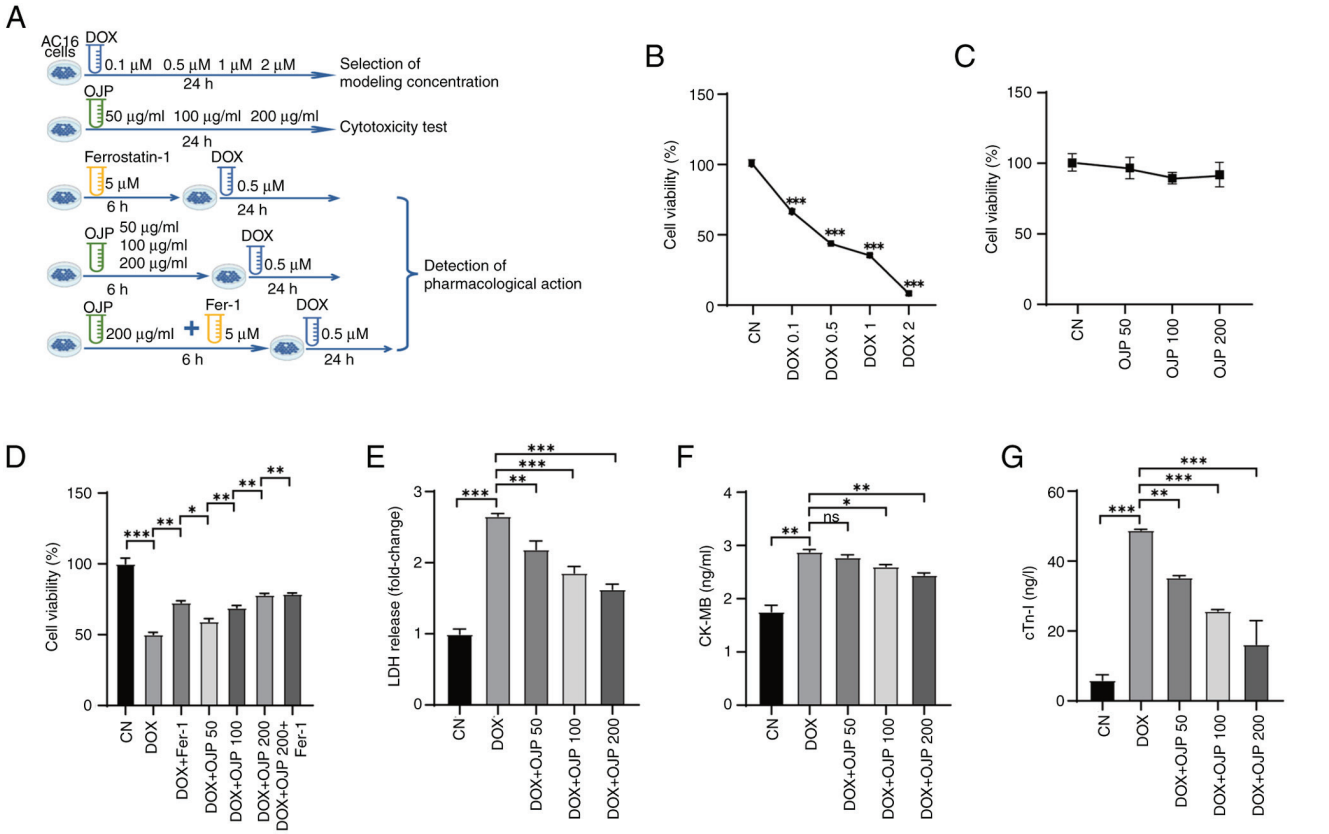

Figure 1. OJP protects AC16 cells against DOX-induced injury. (A) Experimental grouping. Effect of (B) DOX and (C) OJP on cell viability. (D) Effect of OJP on cell viability in DOX-induced myocardial injury cells. Effect of OJP on (E) LDH release, (F) CK-MB and (G) cTn-I in DOX-induced myocardial injury cells. *P<0.05, **P<0.01, ***P<0.001. CK-MB, creatine phosphokinase-MB; CN, control; cTn-I, cardiac troponin I; DOX, doxorubicin; Fer-1, ferrostatin-1; LDH, lactate dehydrogenase; ns, not significant; OJP, *Ophiopogon japonicus* polysaccharide.

death and induced concentration-dependent partial recovery of cell viability. The effect of OJP with Fer-1 suggested that OJP could serve a role in reducing ferroptosis. To evaluate the protective effects of OJP against DIC, the levels of the myocardial injury-related biomarkers LDH, CK-MB and cTn-I were measured. DOX-induced myocardial cell damage was demonstrated by the increased levels of the aforementioned biomarkers. However, OJP at concentrations ranging from 50 to 200 μg/ml decreased the secretion levels of LDH and cTn-I, in a dose-dependent manner, with the most pronounced effect observed at 200 μg/ml (Fig. 1E and G). OJP could alleviate the increase of CK-MB, with a significant effect observed at 200 μg/ml. Although the effect at 50 μg/ml was not statistically significant, it still showed a trend towards alleviation (Fig. 1F). Collectively, the aforementioned findings suggested that OJP could mitigate DOX-induced myocardial damage in a concentration-dependent manner, highlighting its potential as a candidate drug for ameliorating DOX-induced myocardial injury.

OJP alleviates oxidative damage in DOX-induced myocardial ferroptosis. To determine whether OJP decreases lipid peroxidation, changes in the content of GPX4 were assessed. GPX4 serves both as a ferroptosis marker and a crucial endogenous antioxidant enzyme (21). DOX notably downregulated GPX4, thus indicating ferroptosis. OJP partially restored GPX4 expression levels, with the most notable recovery observed in the 200 μg/ml group (Fig. 2A and B). Subsequently, changes in MDA levels were assessed. MDA, the ultimate metabolite of lipid peroxidation, is widely used as a standard marker for assessing the degree of lipid peroxidation (19,22). DOX promoted the production of MDA, whereas cell treatment with OJP significantly reduced MDA content in a concentration-dependent manner (Fig. 2C). In addition, DOX induced severe oxidative stress, as evidenced by the notable increase in green fluorescence, indicating ROS accumulation. However, OJP gradually attenuated the levels of green fluorescence, with those in the 200 μg/ml group almost returning to those observed in the control group (Fig. 2D and E). These results indicated that OJP could upregulate GPX4 and alleviate lipid peroxidation in myocardial ferroptosis in a concentration-dependent manner.

OJP decreases iron accumulation in DOX-induced myocardial ferroptosis. The effect of OJP on iron accumulation in DOX-induced myocardial ferroptosis was evaluated by measuring the expression levels of TFR1 and relative content of Fe^{2+}. Following cell induction with 0.5 μM DOX for 24 h, the protein expression levels of TFR1 were increased, and these were then markedly diminished in OJP-treated cells compared with the DOX group. The most pronounced decrease was observed in the highest OJP dose group (Fig. 3A and B). Fe^{2+} content serves as an indicator of iron accumulation (10). In the DOX group, the FerroOrange

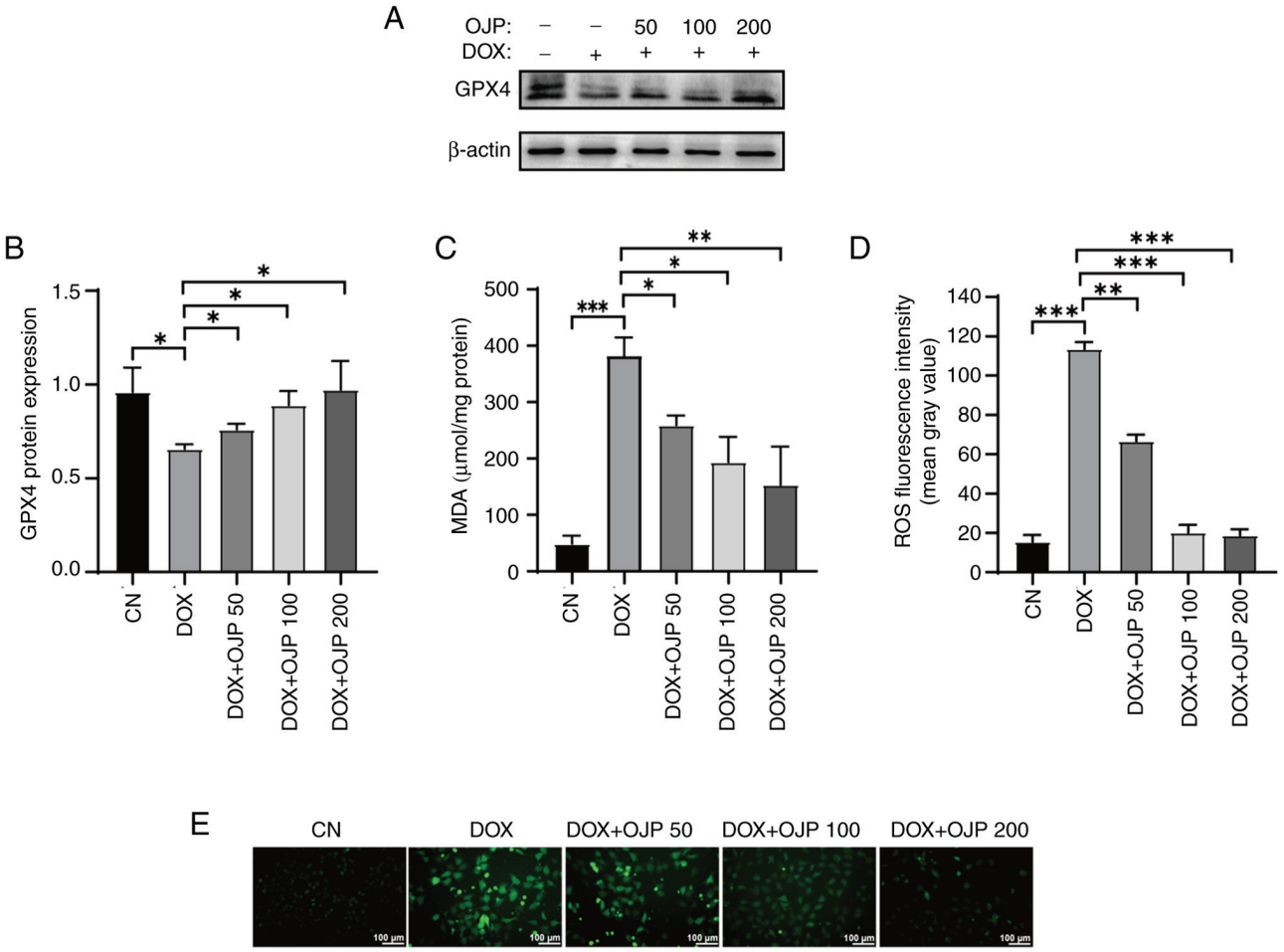

Figure 2. OJP alleviates oxidative damage in DOX-induced myocardial ferroptosis. (A) Western blot bands showing (B) GPX4 protein expression. (C) Effects of OJP on the levels of MDA. (D) ROS fluorescence intensity analysis and (E) representative images. Scale bar, 100 μm. *P<0.05, **P<0.01, ***P<0.001. CN, control; DOX, doxorubicin; GPX4, glutathione peroxidase 4; MDA, malondialdehyde; OJP, *Ophiopogon japonicus* polysaccharide; ROS, reactive oxygen species.

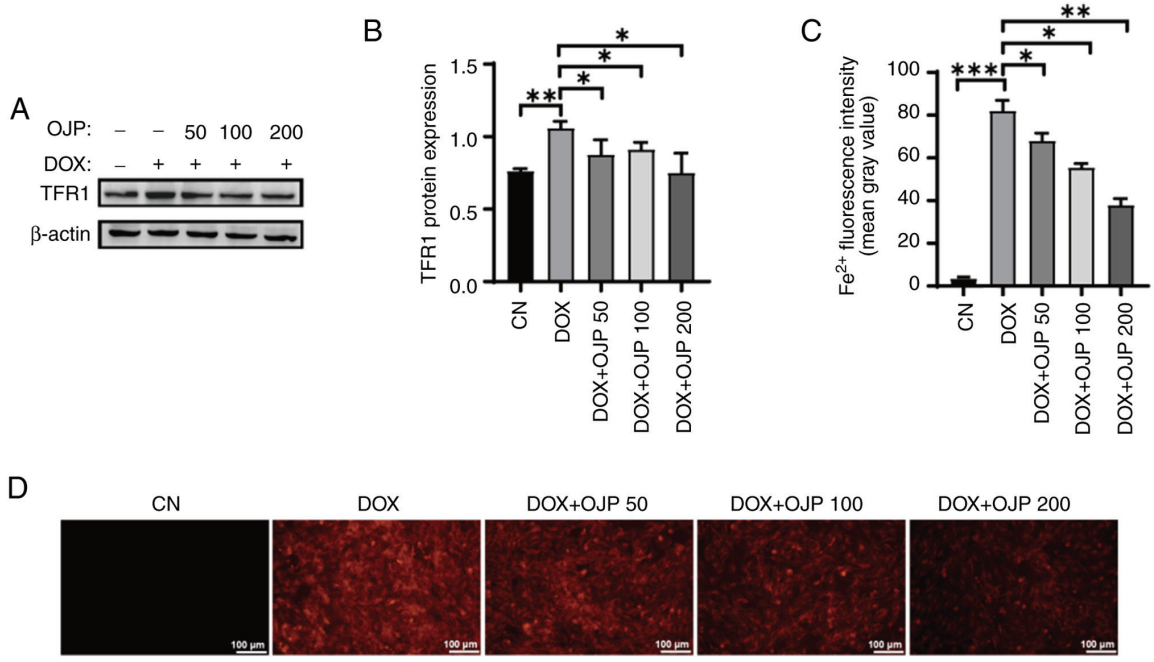

Figure 3. OJP decreases iron accumulation in DOX-induced myocardial ferroptosis. (A) Western blot bands showing (B) TFR1 protein expression. (C) Quantification of Fe^{2+} fluorescence intensity and (D) representative fluorescence images. Scale bar, 100 μm. *P<0.05, **P<0.01, ***P<0.001. CN, control; DOX, doxorubicin; OJP, *Ophiopogon japonicus* polysaccharide; TFR1, transferrin receptor protein 1.

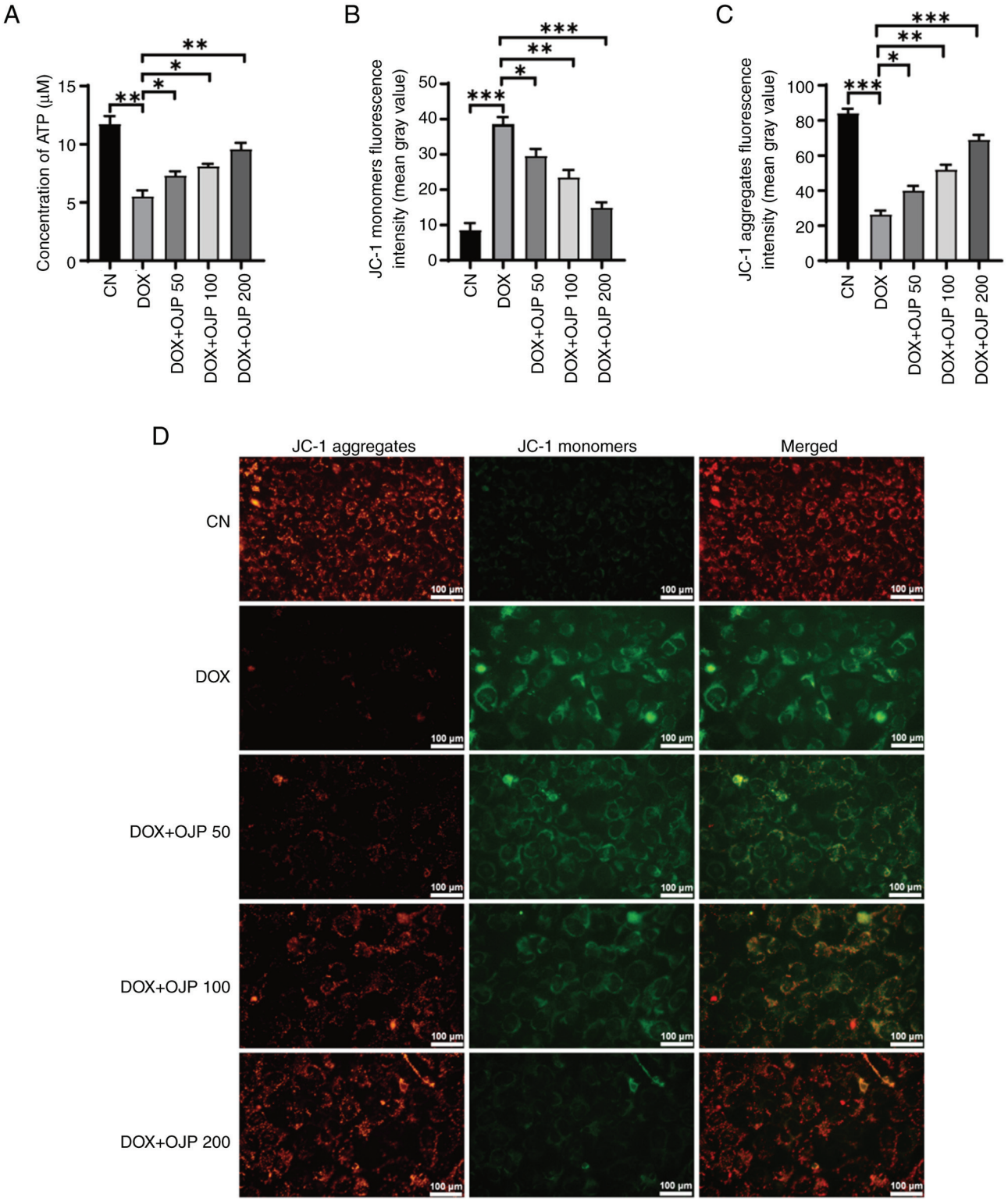

Figure 4. OJP relieves mitochondrial damage in DOX-induced myocardial ferroptosis. (A) Concentration of ATP. (B) JC-1 monomers and (C) JC-1 aggregate fluorescence intensity analysis. (D) Mitochondrial membrane potential representative fluorescence images. Scale bar, 100 μm. *P<0.05, **P<0.01, ***P<0.001. CN, control; DOX, doxorubicin; OJP, *Ophiopogon japonicus* polysaccharide.

probe exhibited bright orange fluorescence upon binding with Fe^{2+} (Fig. 3C and D). Following OJP treatment, the orange fluorescence intensity was significantly decreased in a concentration-dependent manner, thus indicating a notable reduction in intracellular Fe^{2+} content. Taken together, the aforementioned results suggested that OJP downregulated TFR1 and alleviated iron accumulation in DOX-induced myocardial ferroptosis.

OJP relieves mitochondrial dysfunction in DOX-induced myocardial ferroptosis. The onset of ferroptosis commonly coincides with mitochondrial dysfunction, where alterations

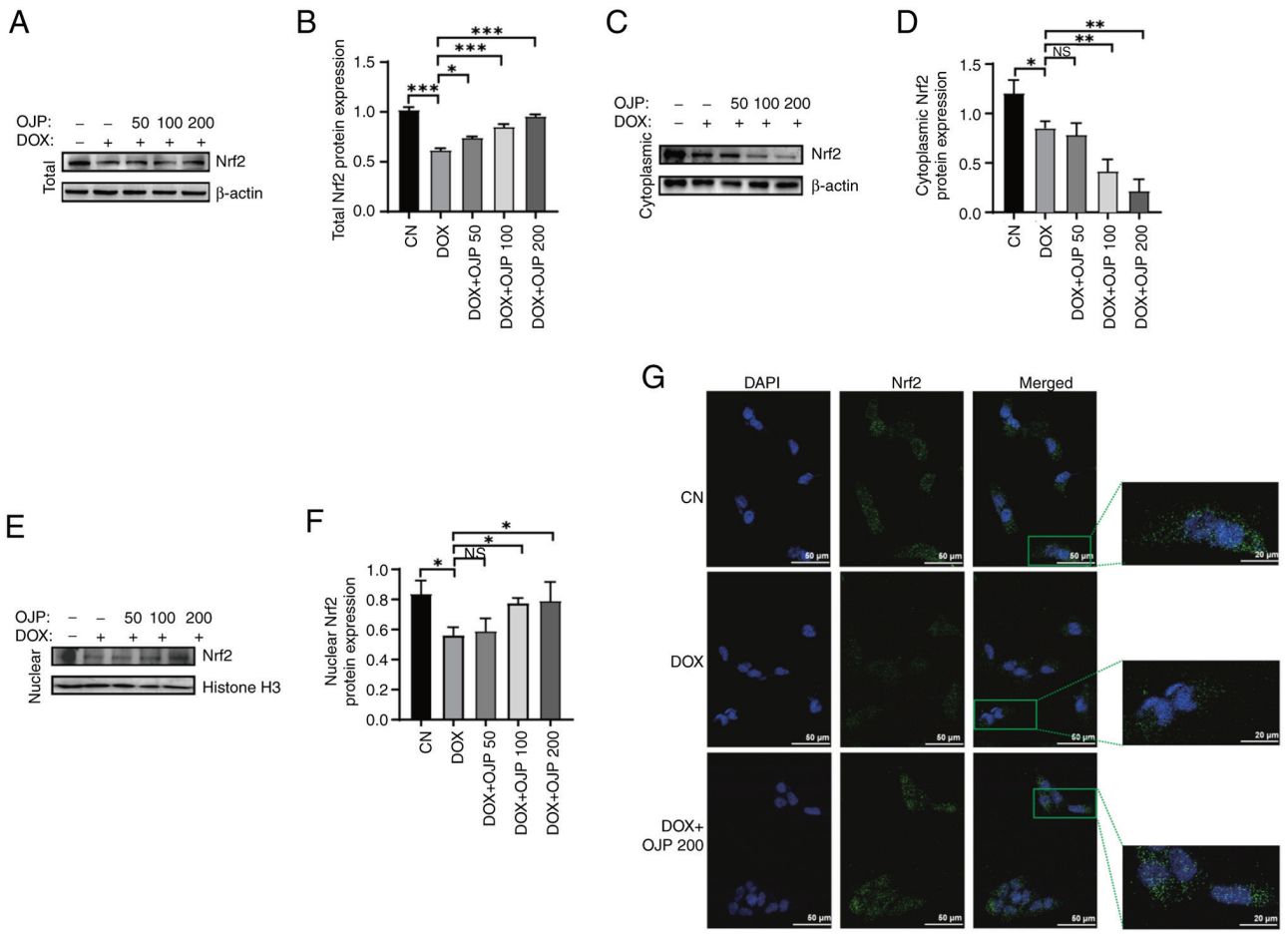

Figure 5. OJP enhances total Nrf2 protein expression and promote its nuclear translocation. (A) Western blot bands showing (B) total Nrf2 protein expression. (C) Protein expression of (D) cytoplasmic Nrf2. (E) Protein expression of (F) nuclear Nrf2. (G) Nrf2 representative immunofluorescence images. Scale bar, 50 or 20 μm. *P<0.05, **P<0.01, ***P<0.001. CN, control; DOX, doxorubicin; Nrf2, nuclear factor erythroid 2-related factor 2; NS, not significant; OJP, *Ophiopogon japonicus* polysaccharide.

in ATP generation and the MMP serve as indicators of mitochondrial performance, indirectly reflecting the extent of ferroptosis (23). DOX decreased ATP production compared with the control group, which was restored in the OJP groups in a concentration-dependent manner (Fig. 4A). In the MMP assessment experiments using JC-1 staining, changes in the fluorescence color of the mitochondrial membrane reflected the degree of mitochondrial injury. The normal control cells exhibited red fluorescence, while those with an impaired mitochondrial membrane exhibited green fluorescence. Green, but not red fluorescence, was prominently observed in cells in the DOX group, thus indicating a decrease in DOX-induced MMP. By contrast, green fluorescence was gradually reduced and red fluorescence was gradually restored in the OJP groups compared with the DOX group, thus indicating an enhanced MMP (Fig. 4B-D). These results suggested that OJP alleviated mitochondrial injury during the progression of myocardial ferroptosis.

OJP attenuates DOX-induced myocardial ferroptosis by enhancing the nuclear translocation of Nrf2. It has been reported that Nrf2 serves a pivotal role in the regulation of ferroptosis (24). To determine the potential mechanism underlying the effect of OJP on myocardial ferroptosis-induced injury, the expression levels of Nrf2 were detected. The protein expression levels of Nrf2 were significantly reduced in the DOX group compared with the control group. Conversely, cell treatment with OJP notably upregulated Nrf2 in a concentration-dependent manner, with 200 μg/ml showing the most pronounced restoring effect (Fig. 5A and B). Given the key role of nuclear translocation in the transcriptional activation of Nrf2 (25), the translocation of Nrf2 was assessed. OJP treatment led to a dose-dependent decrease in cytoplasmic Nrf2 content accompanied by an increase in nuclear Nrf2 accumulation (Fig. 5C-F). The effect of OJP on the Nrf2 pathway was verified via immunofluorescence assays. DOX reduced Nrf2 total and nuclear protein, while OJP could restore Nrf2 expression and promote its nuclear translocation (Fig. 5G). These results suggested that OJP could enhance the total protein levels of Nrf2 and promote its nuclear translocation, thus supporting its potential as a modulator of myocardial ferroptosis. Furthermore, to clarify whether the inhibition of DOX-induced myocardial ferroptosis by OJP is associated with induction of Nrf2 expression, cells were pretreated with the Nrf2 inhibitor ML385 and 200 μg/ml OJP, followed by DOX administration (Fig. 6A). OJP-induced restoration of Nrf2 expression was partially reversed by ML385. In addition, the ability of OJP to upregulate GPX4,

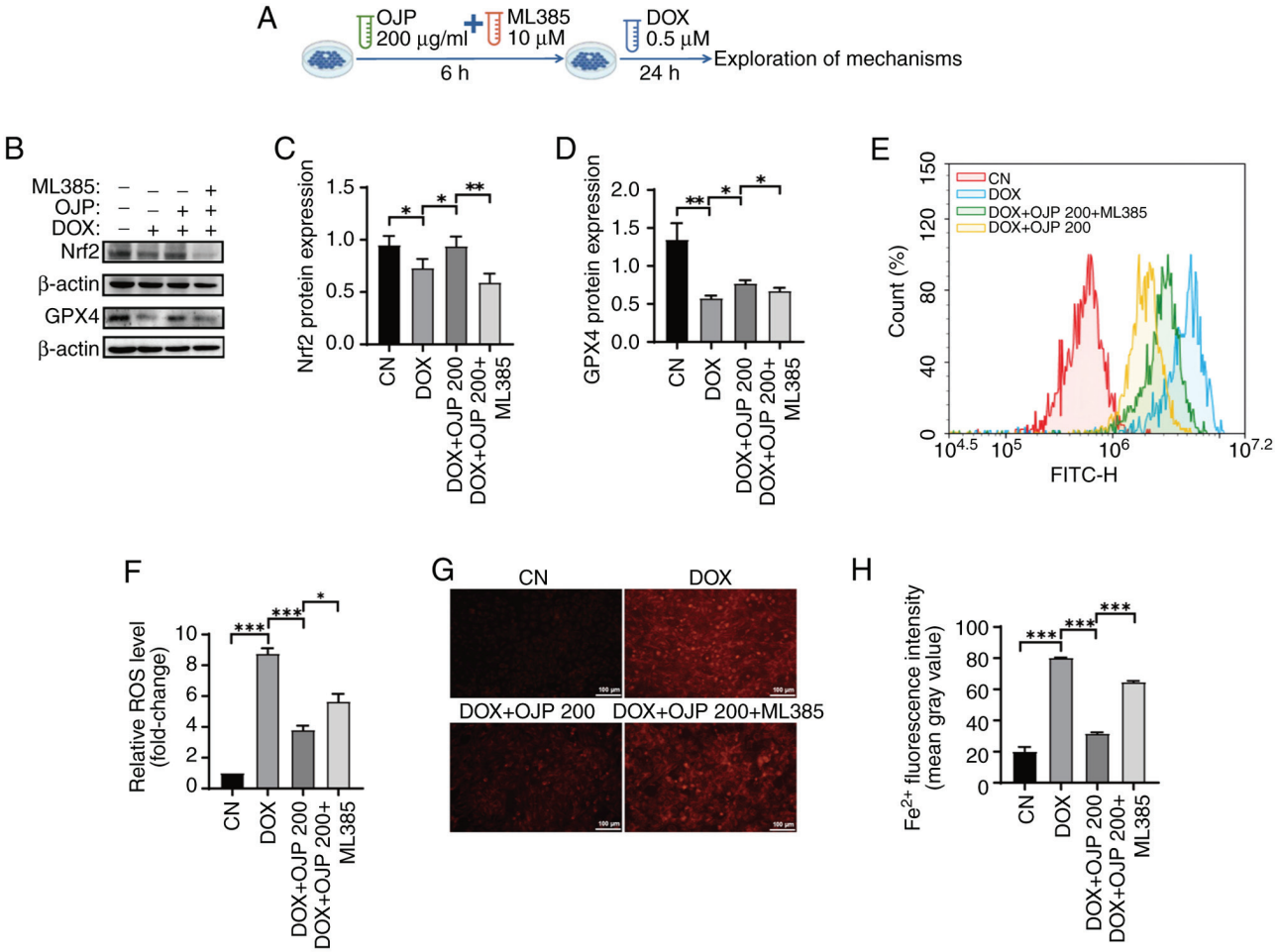

Figure 6. OJP alleviates ROS and iron accumulation in ferroptosis by activating Nrf2. (A) Schematic diagram of the study design. (B) Western blot bands showing (C) Nrf2 and (D) GPX4 protein expression. (E) ROS levels after ML385 treatment by flow cytometry. (F) Analysis of ROS levels by flow cytometry. (G) Representative fluorescence images of (H) Fe^{2+} after addition of ML385. Scale bar, 100 μm. *P<0.05, **P<0.01, ***P<0.001. CN, control; DOX, doxorubicin; GPX4, glutathione peroxidase 4; Nrf2, nuclear factor erythroid 2-related factor 2; OJP, *Ophiopogon japonicus* polysaccharide; ROS, reactive oxygen species.

a downstream signaling molecule of Nrf2 (26), was inhibited by ML385 (Fig. 6B-D). Therefore, the protective effect of OJP against DOX-induced myocardial ferroptosis was partially mediated via enhancing the Nrf2/GPX4 signaling pathway. Nrf2 serves as a regulator of ROS and iron homeostasis via heme metabolism (27). ROS and Fe^{2+} levels were measured to assess whether the OJP-mediated reduction of oxidative stress and iron accumulation in ferroptosis depended on Nrf2 activation. Consistent with aforementioned results, OJP significantly attenuated ROS and Fe^{2+} levels compared with those in the DOX group. ML385 markedly reversed the ability of OJP to reduce ROS and Fe^{2+} levels compared with those in the OJP group (Fig. 6E-H). MDA and MMP levels were determined to evaluate whether OJP relieved DOX-induced lipid peroxidation and mitochondrial injury by enhancing the nuclear translocation of Nrf2. ML385 significantly reduced the ability of OJP to alleviate lipid peroxidation and restore the MMP (Fig. 7A-D). These findings suggested that OJP mitigated DOX-induced ferroptosis in cardiomyocytes by promoting nuclear translocation of Nrf2. Collectively, the aforementioned findings suggested the protective effect of OJP against myocardial ferroptosis was primarily triggered by Nrf2 upregulation.

Discussion

The present study demonstrated that OJP alleviated myocardial ferroptosis by reducing iron accumulation and ROS production, reinstating lipid metabolism and maintaining mitochondrial function. OJP counteracted myocardial ferroptosis via nuclear translocation of Nrf2. The pharmacological effects of OJP could ultimately protect cardiomyocytes from DOX-induced myocardial ferroptosis-triggered injury. The proposed framework of the protective mechanism of OJP against DOX-induced myocardial ferroptosis is depicted in Fig. 8.

The adverse effects of DOX restrict its clinical application and lead to severe heart failure (28). Although dexrazoxane is currently the only drug approved by the US Food and Drug Administration for prevention of DIC in patients with cancer (29), its clinical application is limited by its side effects, including vomiting, dermatitis, subcutaneous necrosis, metabolic abnormality and bone marrow suppression (29). Therefore, the development of novel drugs or strategies for preventing DIC is of importance. Natural compounds are receiving increasing attention due to their lower incidence of side effects and adverse reactions (30). It has been reported

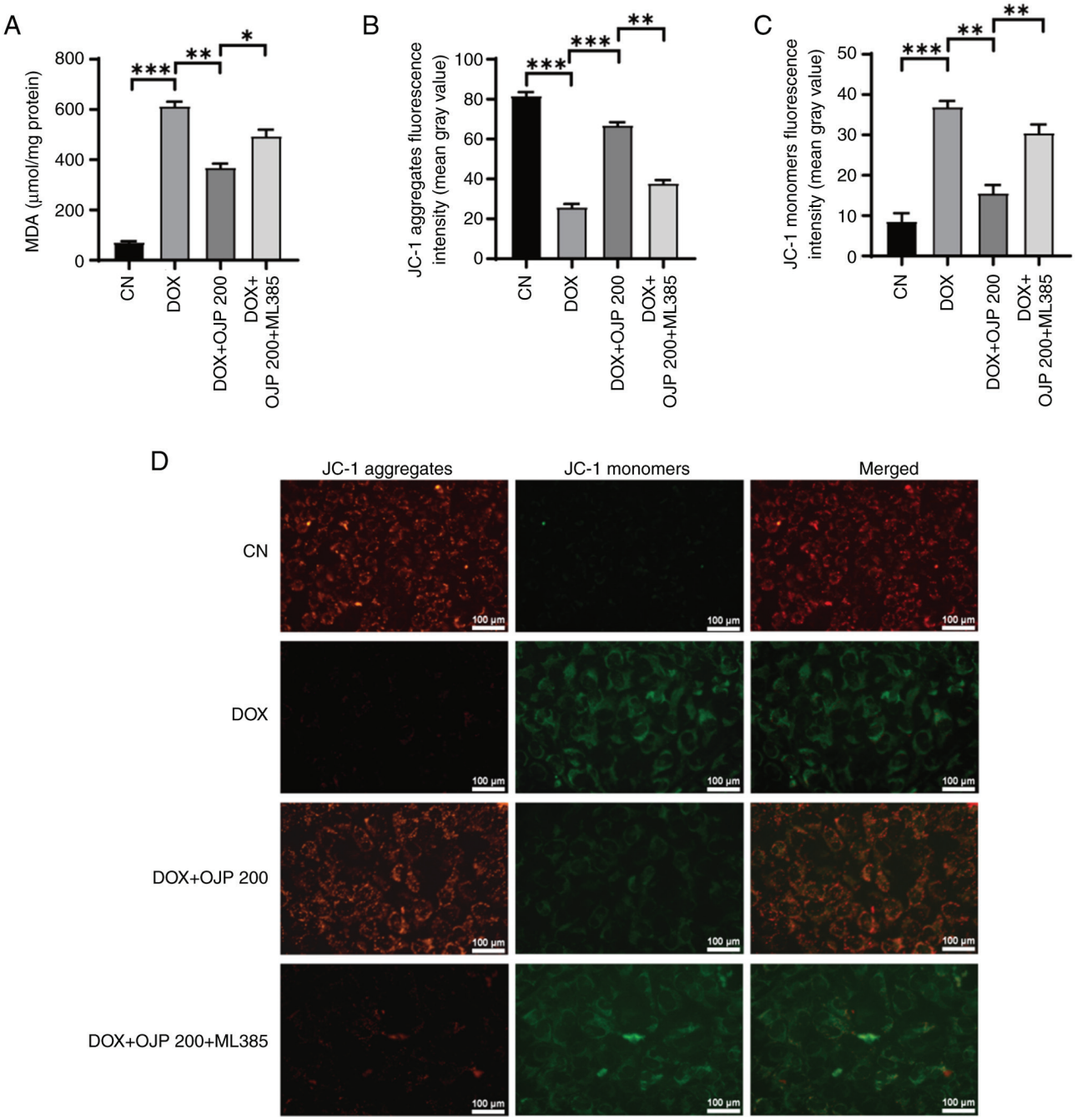

Figure 7. OJP decreases lipid peroxidation and mitochondrial damage in ferroptosis by activating Nrf2. (A) Effects of OJP on the levels of MDA following the addition of ML385. (B) JC-1 aggregates and (C) JC-1 monomers fluorescence intensity analysis following the addition of ML385. (D) Mitochondrial membrane potential representative fluorescence images. Scale bar, 100 μm. *P<0.05, **P<0.01, ***P<0.001. CN, control; DOX, doxorubicin; MDA, malondialdehyde; OJP, *Ophiopogon japonicus* polysaccharide.

that OJP displays therapeutic efficacy against myocardial infarction (31), ischemia-reperfusion injury (32) and diabetic cardiomyopathy (18).

Zhang *et al* (18) found that OJP, when used to treat myocardial injury associated with diabetes, also decreased blood glucose levels and hepatic and renal indices in diabetic rats. Further research has shown that OJP could alleviate lipid accumulation, hepatic degeneration and inflammation in non-alcoholic fatty liver disease (33). OJP has also been shown to protect the integrity of the intestinal epithelial barrier and prevent inflammation-induced epithelial damage (34). Additionally, ophiopogonin D, extracted from *O. japonicus*, has been shown to improve renal function in diabetic rats (35). The aforementioned studies suggest that OJP exerts protective effects across multiple systems in the body without notable toxic or adverse effects. Traditional Chinese medicine formulations containing *O. japonicus* have been applied in clinical practice. For example, Yang *et al* (35) collected data from 110 patients with non-small cell lung cancer and found that, compared with chemotherapy with gemcitabine and cisplatin alone, the combination of Shashen Maidong Decoction (SMD, consists of Adenophora stricta, Polygonatum odoratum,

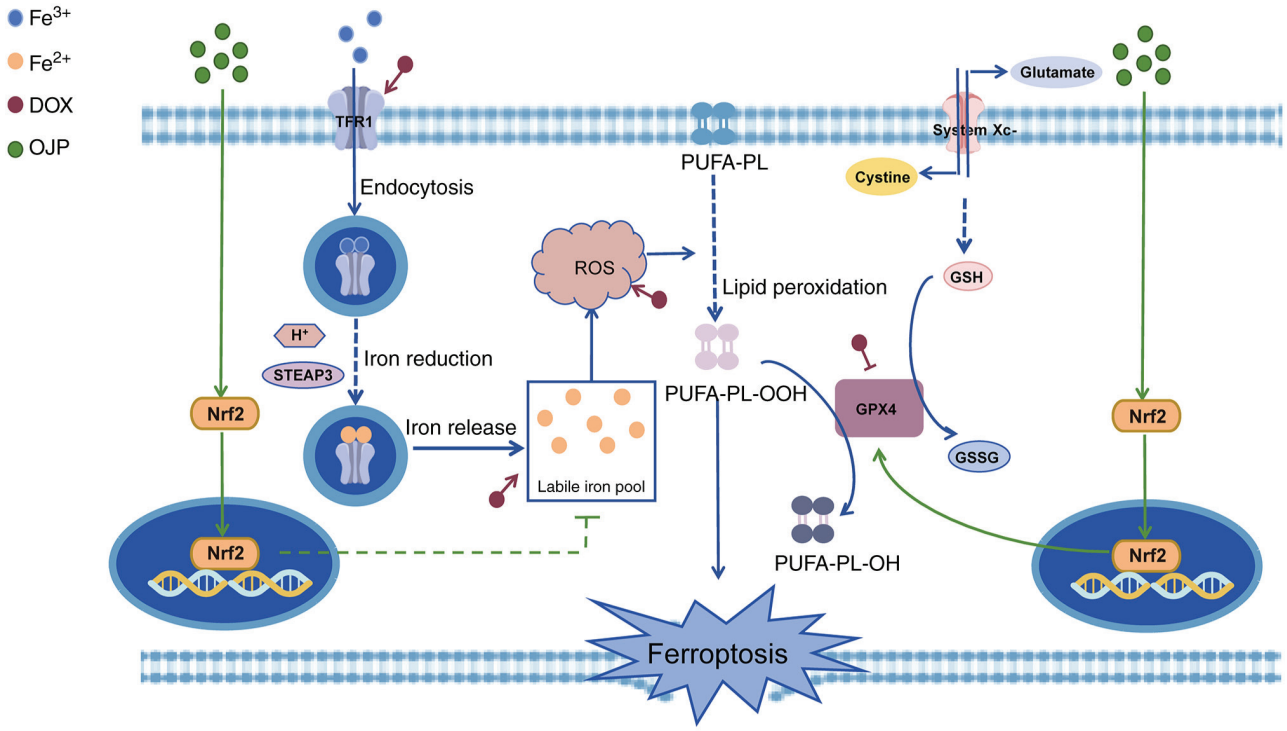

Figure 8. Pharmacological effects and mechanism of OJP attenuating DOX-induced myocardial ferroptosis injury. By promoting the nuclear translocation of Nrf2, OJP reduces the accumulation of labile iron pools and the production of ROS. Additionally, it mitigates lipid peroxidation by enhancing the expression of GPX4, ultimately leading to a decrease in the occurrence of ferroptosis. DOX, doxorubicin; GPX4, glutathione peroxidase 4; GSH, glutathione; GSSG, oxidized glutathione; Nrf2, nuclear factor erythroid 2-related factor 2; OJP, *Ophiopogon japonicus* polysaccharide; PUFA-PL, polyunsaturated fatty acid-phospholipid; ROS, reactive oxygen species; STEAP3, 6-transmembrane epithelial antigen of prostate 3; TFR1, transferrin receptor protein 1.

Glycyrrhiza uralensis, Morus alba, O. japonicus, Lablab purpureus, and Trichosanthes kirilowii) with chemotherapy led to a greater decrease in inflammation levels. Additionally, the clinical efficacy was higher, as evidenced by an improved Karnofsky performance status score, increased body weight stability and a lower incidence of adverse reactions. Although there are no clinical reports on the use of *O. japonicus* alone (36), the application of traditional Chinese medicine formulas containing *O. japonicus* highlights its advantages both in terms of clinical efficacy and safety.

The present study also further verified that OJP could significantly improve DOX-induced cardiomyocyte failure, evidenced by the enhanced viability of cardiomyocytes and decreased levels of the myocardial injury-related markers LDH, CK-MB and cTn-I. Furthermore, OJP did not display cytotoxic effects at the administered doses. These findings suggest that OJP may serve as a promising candidate drug with improved safety and fewer side effects for mitigating DOX-induced cardiomyocyte injury, thereby delaying progression of myocardial damage.

The involvement of ferroptosis in the pathogenesis of DIC has been supported by a previous study (37). Therefore, the present study aimed to explore whether the protective effects of OJP on cardiomyocytes were mediated by reducing ferroptosis. Ferroptosis is characterized by iron accumulation and redox system dysregulation (38). Fan *et al* (39) demonstrated that OJP mitigated isoproterenol-induced myocardial injury by enhancing the expression of free radical scavenging enzymes, such as superoxide dismutase and catalase. Consistently, the present study revealed that OJP upregulated GPX4 and mitigated DOX-induced oxidative stress and lipid peroxidation, supporting its potential in alleviating DOX-induced myocardial ferroptosis by enhancing the antioxidant system.

Excessive iron accumulation in the body forms the labile iron pool, eventually promoting ferroptosis (40). However, to the best of our knowledge, there is limited research on the role of OJP in modulating iron accumulation (16). To the best of our knowledge, the present study was the first to demonstrate that cell treatment with OJP significantly decreased the expression of the iron transport protein TFR1. Furthermore, intracellular Fe^{2+} content was notably decreased in the OJP groups, thus inhibiting intracellular iron buildup. Ferroptosis disrupts the mitochondrial balance, thus leading to mitochondrial injury (41). In the present study, OJP administration partially restored mitochondrial function and decreased mitochondrial injury. These observations underscore the potential of OJP as a promising therapeutic agent for managing and preventing DOX-induced myocardial ferroptosis.

The signaling pathways of ferroptosis are intricate, affecting cellular antioxidant capacity and resulting in lipid peroxidation (38). Nrf2 is a key regulator of antioxidant responses, serving a crucial role in maintaining cellular redox homeostasis (25). GPX4, a downstream target of Nrf2, serves a key role in inhibiting ferroptosis by catalyzing the reduction of lipid peroxides using glutathione (42). The excessive accumulation of Fe^{2+} leads to increased lipid peroxidation (43). It has been reported that Nrf2 stabilizes intracellular iron homeostasis by regulating the expression of heme metabolism-related proteins and the heavy and light chains of ferritin, thus indirectly

regulating Fe^{2+} levels in the labile iron pool (44). For example, previous studies have indicated that dexmedetomidine and naringenin decreased myocardial ischemia/reperfusion-induced ferroptosis by upregulating Nrf2 (45,46). Similarly, prostaglandin E2 receptor 1, astragaloside IV and fisetin protect cardiomyocytes against DOX-induced ferroptosis via activation of Nrf2 signaling (15,47,48). Conversely, Wang *et al* (49) demonstrated that Nrf2 inhibition aggravated myocardial injury. OJP has significant cardiovascular protective effects due to its anti-inflammatory and antioxidant properties (50), suggesting that Nrf2 may play a crucial role in these mechanisms. As a key intracellular antioxidant transcription factor, Nrf2 provides critical protection against oxidative stress (51). OJP may activate the Nrf2 signaling pathway, enhancing the activity of antioxidant enzymes and reducing lipid peroxidation, thereby mitigating ferroptosis-induced myocardial damage. Furthermore, Nrf2 regulates genes involved in iron metabolism, aiding in the maintenance of intracellular iron homeostasis and reducing oxidative stress and cellular injury caused by iron overload (43). In the aforementioned study, OJP could increase the protein expression levels of Nrf2 and promote its nuclear translocation. To ascertain whether Nrf2 inhibition abrogated the protective effect of OJP, ML385, an Nrf2 inhibitor, was employed. ML385 not only suppressed OJP-mediated upregulation of Nrf2 and its downstream target GPX4, but also reversed the effect of OJP in reducing mitochondrial injury and iron accumulation. These findings supported the anti-ferroptosis mechanism of OJP via regulation of the Nrf2/GPX4 signaling pathway and decreasing iron accumulation.

However, the present study has some limitations. Firstly, only the expression levels of core proteins of the downstream GPX4 signaling pathway and those involved in regulation of Fe^{2+} production were detected. Second, the present study did not investigate how Nrf2 indirectly regulates TFR1, leaving the intricate molecular pathways involved for future exploration. Lastly, the specific molecular mechanisms by which OJP alleviates mitochondrial damage were not thoroughly examined. Therefore, the detailed molecular mechanisms underlying the regulation of Nrf2 signaling during OJP-mediated protection against ferroptosis should be further investigated. Subsequent studies should assess the particular activation mechanisms of the Nrf2 signaling pathway by OJP and its effects on downstream molecular targets.

The present study provided novel insights into the favorable pharmacological effects of OJP against DOX-induced myocardial ferroptosis and its underlying mechanisms, thus laying the groundwork for the future development of novel therapeutic strategies for the prevention and treatment of DOX-induced myocardial disease. OJP could be considered as a promising candidate for potential clinical intervention.

Acknowledgements

Not applicable.

Funding

The present study was supported by Research Project of Health Commission of Pudong New Area, Shanghai (grant no. PW2021A-69), Clinical Research Center, Shanghai University of Medicine & Health Sciences (grant no. 22MC2022002) and Research Grant for Pudong Health Bureau of Shanghai (grant no. YC-2023-0401).

Availability of data and materials

The data generated in the present study may be requested from the corresponding author.

Authors' contributions

YC performed experiments, analyzed the data and wrote the manuscript. LM analyzed data and revised the manuscript. XW and LC performed experiments and data analysis. ML designed the study and revised the manuscript. YL and YY analyzed data. All authors have read and approved the final manuscript. YL and ML confirm the authenticity of all the raw data.

Ethics approval and consent to participate

Not applicable.

Patient consent for publication

Not applicable.

Competing interests

The authors declare that they have no competing interests.

References

1. Rawat PS, Jaiswal A, Khurana A, Bhatti JS and Navik U: Doxorubicin-induced cardiotoxicity: An update on the molecular mechanism and novel therapeutic strategies for effective management. Biomed Pharmacother 139: 111708, 2021.
2. Liu C, Ma X, Zhuang J, Liu L and Sun C: Cardiotoxicity of doxorubicin-based cancer treatment: What is the protective cognition that phytochemicals provide us? Pharmacol Res 160: 105062, 2020.
3. Jones IC and Dass CR: Doxorubicin-induced cardiotoxicity: Causative factors and possible interventions. Pharm Pharmacol 74: 1677-1688, 2022.
4. Carvalho C, Santos RX, Cardoso S, Correia S, Oliveira PJ, Santos MS and Moreira PI: Doxorubicin: The good, the bad and the ugly effect. Curr Med Chem 16: 3267-3285, 2009.
5. Christiansen S and Autschbach R: Doxorubicin in experimental and clinical heart failure. Eur J Cardiothorac Surg 30: 611-616, 2006.
6. Hardaway BW: Adriamycin-associated cardiomyopathy: where are we now? updates in pathophysiology, dose recommendations, prognosis, and outcomes. Curr Opin Cardiol 34: 289-295, 2019.
7. Stockwell BR: Ferroptosis turns 10: Emerging mechanisms, physiological functions, and therapeutic applications. Cell 185: 2401-2421, 2022.
8. Fujii J, Homma T and Kobayashi S: Ferroptosis caused by cysteine insufficiency and oxidative insult. Free Radic Res 54: 969-980, 2020.
9. Kotamraju S, Chitambar CR, Kalivendi SV, Joseph J and Kalyanaraman B: Transferrin receptor-dependent iron uptake is responsible for doxorubicin-mediated apoptosis in endothelial cells: Role of oxidant-induced iron signaling in apoptosis. J Biol Chem 277: 17179-17187, 2002.
10. Fang X, Ardehali H, Min J and Wang F: The molecular and metabolic landscape of iron and ferroptosis in cardiovascular disease. Nat Rev Cardiol 20: 7-23, 2023.

11. Dixon SJ, Lemberg KM, Lamprecht MR, Skouta R, Zaitsev EM, Gleason CE, Patel DN, Bauer AJ, Cantley AM, Yang WS, *et al*: Ferroptosis: an iron-dependent form of nonapoptotic cell death. Cell 149: 1060-1072, 2012.
12. Lu J, Zhao Y, Liu M, Lu J and Guan S: Toward improved human health: Nrf2 plays a critical role in regulating ferroptosis. Food Funct 12: 9583-9606, 2021.
13. Luo LF, Guan P, Qin LY, Wang JX, Wang N and Ji ES: Astragaloside IV inhibits adriamycin-induced cardiac ferroptosis by enhancing Nrf2 signaling. Mol Cell Biochem 476: 2603-2611, 2021.
14. Yu W, Chen C, Xu C, Xie D, Wang Q, Liu W, Zhao H, He F, Chen B, Xi Y, *et al*: Activation of p62-NRF2 axis protects against doxorubicin-induced ferroptosis in cardiomyocytes: A novel role and molecular mechanism of resveratrol. Am J Chin Med 50: 2103-2123, 2022.
15. Li D, Liu X, Pi W, Zhang Y, Yu L, Xu C, Sun Z and Jiang J: Fisetin attenuates doxorubicin-induced cardiomyopathy in vivo and in vitro by inhibiting ferroptosis through SIRT1/Nrf2 signaling pathway activation. Front Pharmacol 12: 808480, 2022.
16. Fang J, Wang X, Lu M, He X and Yang X: Recent advances in polysaccharides from Ophiopogon japonicus and Liriope spicata var. prolifera. Int J Biol Macromol 114: 1257-1266, 2018.
17. Chen MH, Chen XJ, Wang M, Lin LG and Wang YT: Ophiopogon japonicus-A phytochemical, ethnomedicinal and pharmacological review. J Ethnopharmacol 181: 193-213, 2016.
18. Zhang J, Fan S, Mao Y, Ji Y, Jin L, Lu J and Chen X: Cardiovascular protective effect of polysaccharide from Ophiopogon japonicus in diabetic rats. Int J Biol Macromol 82: 505-513, 2016.
19. Ayala A, Muñoz MF and Argüelles S: Lipid peroxidation: production, metabolism, and signaling mechanisms of malondialdehyde and 4-hydroxy-2-nonenal. Oxid Med Cell Longev 2014: 360438, 2014.
20. Cao Y, Shen T, Huang X, Lin Y, Chen B, Pang J, Li G, Wang Q, Zohrabian S, Duan C, *et al*: Astragalus polysaccharide restores autophagic flux and improves cardiomyocyte function in doxorubicin-induced cardiotoxicity. Oncotarget 8: 4837-4848, 2017.
21. Xie Y, Kang R, Klionsky DJ and Tang D: GPX4 in cell death, autophagy, and disease. Autophagy 19: 2621-2638, 2023.
22. Tsikas D: Assessment of lipid peroxidation by measuring malondialdehyde (MDA) and relatives in biological samples: Analytical and biological challenges. Anal Biochem 524: 13-30, 2017.
23. Otasevic V, Vucetic M, Grigorov I, Martinovic V and Stancic A: Ferroptosis in different pathological contexts seen through the eyes of mitochondria. Oxid Med Cell Longev 2021: 5537330, 2021.
24. Dodson M, Castro-Portuguez R and Zhang DD: NRF2 plays a critical role in mitigating lipid peroxidation and ferroptosis. Redox Biol 23: 101107, 2019.
25. He F, Ru X and Wen T: NRF2, a transcription factor for stress response and beyond. Int J Mol Sci 21: 4777, 2020.
26. Jiang X, Yu M, Wang WK, Zhu LY, Wang X, Jin HC and Feng LF: The regulation and function of Nrf2 signaling in ferroptosis-activated cancer therapy. Acta Pharmacol Sin 45: 2229-2240, 2024.
27. Fang X, Wang H, Han D, Xie E, Yang X, Wei J, Gu S, Gao F, Zhu N, Yin X, *et al*: Ferroptosis as a target for protection against cardiomyopathy. Proc Natl Acad Sci USA 116: 2672-2680, 2019.
28. Prathumsap N, Shinlapawittayatorn K, Chattipakorn SC and Chattipakorn N: Effects of doxorubicin on the heart: From molecular mechanisms to intervention strategies. Eur J Pharmacol 866: 172818, 2020.
29. Cvetković RS and Scott LJ: Dexrazoxane: A review of its use for cardioprotection during anthracycline chemotherapy. Drugs 65: 1005-1024, 2005.
30. Zhou D, Zhang H, Xue X, Tao Y, Wang S, Ren X and Su J: Safety evaluation of natural drugs in chronic skeletal disorders: A literature review of clinical trials in the past 20 years. Front Pharmacol 12: 801287, 2022.
31. Wang S, Lin X, Wang LY, Ruan KF, Feng Y and Li XY: A polysaccharides MDG-1 augments survival in the ischemic heart by inducing S1P release and S1P1 expression. Int J Biol Macromol 50: 734-740, 2012.
32. Zheng Q, Feng Y, Xu DS, Lin X and Chen YZ: Influence of sulfation on anti-myocardial ischemic activity of Ophiopogon japonicus polysaccharide. J Asian Nat Prod Res 11: 306-321, 2009.
33. Zhang L, Wang Y, Wu F, Wang X, Feng Y and Wang Y: MDG, an Ophiopogon japonicus polysaccharide, inhibits non-alcoholic fatty liver disease by regulating the abundance of Akkermansia muciniphila. Int J Biol Macromol 196: 23-34, 2022.
34. Lin C, Kuo TC, Lin JC, Ho YC and Mi FL: Delivery of polysaccharides from Ophiopogon japonicus (OJPs) using OJPs/chitosan/whey protein co-assembled nanoparticles to treat defective intestinal epithelial tight junction barrier. Int J Biol Macromol 160: 558-570, 2020.
35. Yang ZG, Liang X and Zhao YQ: Effect of shashen maidong tang combined with chemotherapy on immune function and inflammatory reaction of patients with lung cancer of Qi and Yin deficiency. Chin J Exp Tradit Med 23: 158-163, 2017 (In Chinese).
36. Yue L, Xiao L, Zhang X, Niu L, Wen Y, Li X, Wang Y, Xing G and Li G: Comparative efficacy of Chinese herbal injections in patients with cardiogenic shock (CS): A systematic review and Bayesian network meta-analysis of randomized controlled trials. Front Pharmacol 15: 1348360, 2024.
37. Tadokoro T, Ikeda M, Ide T, Deguchi H, Ikeda S, Okabe K, Ishikita A, Matsushima S, Koumura T, Yamada KI, *et al*: Mitochondria-dependent ferroptosis plays a pivotal role in doxorubicin cardiotoxicity. JCI Insight 8: e169756, 2023.
38. Su LJ, Zhang JH, Gomez H, Murugan R, Hong X, Xu D, Jiang F and Peng ZY: Reactive oxygen species-induced lipid peroxidation in apoptosis, autophagy, and ferroptosis. Oxid Med Cell Longev 2019: 5080843, 2019.
39. Fan S, Zhang J, Xiao Q, Liu P, Zhang Y, Yao E and Cahen X: Cardioprotective effect of the polysaccharide from Ophiopogon japonicus on isoproterenol-induced myocardial ischemia in rats. Int J Biol Macromol 147: 233-240, 2020.
40. Dai E, Chen X, Linkermann A, Jiang X, Kang R, Kagan VE, Bayir H, Yang WS, Garcia-Saez AJ, Ioannou MS, *et al*: A guideline on the molecular ecosystem regulating ferroptosis. Nat Cell Biol 26: 1447-1457, 2024.
41. Gao M, Yi J, Zhu J, Minikes AM, Monian P, Thompson CB and Jiang X: Role of mitochondria in ferroptosis. Mol Cell 73: 354-363. e3, 2019.
42. Wang M, Tang J, Zhang S, Pang K, Zhao Y, Liu N, Huang J, Kang J, Dong S, Li H, *et al*: Exogenous H2S initiating Nrf2/GPx4/GSH pathway through promoting Syvn1-Keap1 interaction in diabetic hearts. Cell Death Discov 9: 394, 2023.
43. Kerins MJ and Ooi A: The Roles of NRF2 in modulating cellular iron homeostasis. Antioxid Redox Signal 29: 1756-1773, 2018.
44. Song X and Long D: Nrf2 and Ferroptosis: A new research direction for neurodegenerative diseases. Front Neurosci 14: 267, 2020.
45. Wang Z, Yao M, Jiang L, Wang L, Yang Y, Wang Q, Qian X, Zhao Y and Qian J: Dexmedetomidine attenuates myocardial ischemia/reperfusion-induced ferroptosis via AMPK/GSK-3β/Nrf2 axis. Biomed Pharmacother 154: 113572, 2022.
46. Xu S, Wu B, Zhong B, Lin L, Ding Y, Jin X, Huang Z, Lin M, Wu H and Xu D: Naringenin alleviates myocardial ischemia/reperfusion injury by regulating the nuclear factor-erythroid factor 2-related factor 2 (Nrf2)/System xc-/glutathione peroxidase 4 (GPX4) axis to inhibit ferroptosis. Bioengineered 12: 10924-10934, 2021.
47. Zhang J, Wu C, Gao L, Du G and Qin X: Astragaloside IV derived from Astragalus membranaceus: A research review on the pharmacological effects. Adv Pharmacol 87: 89-112, 2020.
48. Wang B, Jin Y, Liu J, Liu Q, Shen Y, Zuo S and Yu Y: EP1 activation inhibits doxorubicin-cardiomyocyte ferroptosis via Nrf2. Redox Biol 65: 102825, 2023.
49. Wang Y, Yan S, Liu X, Deng F, Wang P, Yang L, Hu L, Huang K and He J: PRMT4 promotes ferroptosis to aggravate doxorubicin-induced cardiomyopathy via inhibition of the Nrf2/GPX4 pathway. Cell Death Differ 29: 1982-1995, 2022.
50. Liu Q, Lu JJ, Hong HJ, Yang Q, Wang Y and Chen XJ: Ophiopogon japonicus and its active compounds: A review of potential anticancer effects and underlying mechanisms. Phytomedicine 113: 154718, 2023.
51. Chen QM and Maltagliati AJ: Nrf2 at the heart of oxidative stress and cardiac protection. Physiol Genomics 50: 77-97, 2018.